Toxicology Research

PAPER

View Article Online
View Journal

Cite this: DOI: 10.1039/c5tx00209e

Promising blood-derived biomarkers for estimation of the *postmortem* interval†

Isabel Costa,[a,b,c] Félix Carvalho,[b] Teresa Magalhães,[c,d] Paula Guedes de Pinho,[b] Ricardo Silvestre*[e,f] and Ricardo Jorge Dinis-Oliveira*[a,b,c,d]

Received 27th June 2015,
Accepted 17th August 2015

DOI: 10.1039/c5tx00209e

www.rsc.org/toxicology

A precise estimation of the *postmortem* interval (PMI) is one of the most important topics in forensic pathology. However, the PMI estimation is based mainly on the visual observation of cadaverous phenomena (*e.g. algor*, *livor* and *rigor mortis*) and on alternative methods such as thanatochemistry that remain relatively imprecise. The aim of this *in vitro* study was to evaluate the kinetic alterations of several biochemical parameters (*i.e.* proteins, enzymes, substrates, electrolytes and lipids) during putrefaction of human blood. For this purpose, we performed kinetic biochemical analysis during a 264 hour period. The results showed a significant linear correlation between total and direct bilirubin, urea, uric acid, transferrin, immunoglobulin M (IgM), creatine kinase (CK), aspartate transaminase (AST), calcium and iron with the time of blood putrefaction. These parameters allowed us to develop two mathematical models that may have predictive values and become important complementary tools of traditional methods to achieve a more accurate PMI estimation.

Introduction

One of the most important and challenging problems for forensic pathologists is the accurate estimation of the *postmortem* interval (PMI).[1] The main subjacent principle is the calculation of a measurable date along a time-dependent curve back to the starting point.[2] All the methods currently used to estimate the PMI are still far from being exact. The physical (*algor mortis*, *livor mortis*) and physicochemical (*rigor mortis*) changes comprise the main basis for PMI estimation, especially during the first hours after death. However, these changes have limitations in PMI determination, due to the bias inflicted by several variables.[3–8] Other methods such as thanatochemistry and molecular techniques have been reported, attempting for a more accurate PMI estimation, but until now all these methods have also been relatively inexact and/or poorly reproducible.[9] Over the last few decades, some progress in PMI estimation has been made using biochemical parameters, supported by different statistical approaches.[9–11] These methods have been shown to be more accurate in PMI estimation, since the effect of external conditions is less relevant than in the currently used traditional methods. Moreover, a combination of traditional and biochemical methods has been proposed to increase the reliability of PMI estimations and narrow down the margins of error associated with individual analysis.[9,12,13] An important feature of biochemical methods is also the possibility of using the results for the accurate estimation of the PMI during the first days after death since most victims are found in the first hours after death.[9] The graphical abstract image summarizes the current methods used for PMI estimation.

An accurate estimation of the PMI requires the evaluation of parameters that correlate with time after death.[14] This definition fits well in *postmortem* changes of biochemical parameters, since each change has its own time factor. These changes begin immediately after death, initiating at the cellular level and subsequently evolving to hemolysis, discoloration, swelling, and putrefaction, among other processes.[15,16] During human decomposition, several biochemical changes take place in all body tissues due to the absence of circulating oxygen and the consequent cessation of aerobic respiration, altered enzymatic reactions, cessation of anabolic production of metabolites, cessation of active membrane transport and changes in the permeability of cells and diffusion of

[a]*IINFACTS – Institute of Research and Advanced Training in Health Sciences and Technologies, Department of Sciences, University Institute of Health Sciences (IUCS), CESPU, CRL, Gandra, Portugal*
[b]*UCIBIO-REQUIMTE, Laboratory of Toxicology, Department of Biological Sciences, Faculty of Pharmacy, University of Porto, Porto, Portugal*
[c]*Department of Legal Medicine and Forensic Sciences, Faculty of Medicine, University of Porto, Porto, Portugal*
[d]*CENCIFOR – Forensic Sciences Center, Coimbra, Portugal.*
E-mail: ricardinis@med.up.pt; Tel: +351 222073850
[e]*Life and Health Sciences Research Institute (ICVS), School of Health Sciences, University of Minho, Braga, Portugal*
[f]*ICVS/3B's – PT Government Associate Laboratory, Braga/Guimarães, Portugal.*
E-mail: ricardosilvestre@ecsaude.uminho.pt; Tel: +351 253604811
†Electronic supplementary information (ESI) available. See DOI: 10.1039/c5tx00209e

ions.[5,17–19] The catabolic activity of key enzymes on proteins, lipids, carbohydrates and nucleic acids and the rate of this process may be used to estimate the PMI.[15,17,19–21] Additionally, the leaching of electrolytes, and blood pH changes, due to accumulation of several ions and metabolites such as bicarbonates, carbon dioxide, hydrogen ions, lactate, phosphoric and formic acids have been suggested as potential targets for PMI determination.[17,22]

Biochemical analysis as a useful indicator for estimating PMI has already been presented by some authors. Data have been reported of a significant correlation between the *postmortem* concentration of some biochemical parameters such as potassium,[1,11,23–25] urea,[26] glucose,[11,23] lactate,[17] hypoxanthine,[17,24,27] glycated hemoglobin,[28] calcineurin A, phosphatase 2A,[8,29] troponin,[30] cytochrome *c* oxidase,[31] lactate and malate dehydrogenase,[32] gamma amino butyric acid[15] and PMI in distinct biological matrices (*e.g.* vitreous humor, blood, cerebrospinal and synovial fluids).

The development of more reliable techniques will certainly represent important tools to be used in the court of law (*e.g.* by inclusion or exclusion of possible suspects).[33] Therefore, this study aims to evaluate the kinetic alterations of 46 biochemical parameters in human blood in order to develop a mathematical model that could be used as a complementary procedure for the methodologies already used. Thus, substrates, proteins, enzymes, electrolytes and lipids are targeted in this study, since these may be useful for rigorous PMI estimation.

Materials and methods

Samples

Twenty independent human venous blood samples (40 mL each) were collected from healthy donors and divided for 16 plastic tubes (*e.g.* without anticoagulants or any other additives), one for each of the defined endpoints (see below). Informed written consent was obtained from the participants. This work was also approved by the Ethical Commission of the Faculty of Medicine of the University of Porto/Saint John Hospital. Whole blood was subjected to a temperature decrease gradually from 37 to 21 °C, mimicking the decline of body temperature after death until it reaches room temperature. According to the literature,[13] there is an initial maintenance of body temperature that may last for a few hours, followed by a relatively linear rate of *postmortem* cooling, until reaching room temperature. Thus, during the first hour, samples were maintained at 37 °C in a thermostatic bath. Then, the temperature was decreased 0.5 °C per hour up to 12 h, 1 °C per hour up to 18 h and 0.5 °C per hour until room temperature was achieved.

Quantitative pH and biochemical parameter kinetic analysis

Determination of the pH and the quantification of the vast biochemical array (46) of different biochemical parameters were performed at 16 defined endpoints to promote hemolysis (1, 4, 8, 12, 14, 24, 48, 72, 96, 120, 144, 168, 192, 216, 240, 264 hours). For that, complete venous blood samples were centrifuged at 3000*g* for 10 min to obtain serum. The following biochemical parameters were quantified in this study using a Prestige 24i® Automated Chemistry Analyzer: substrates [urea, creatinine, uric acid, lactate, glucose, direct bilirubin and total bilirubin (Cormay, Poland)], enzymes [lipase, creatine kinase – (CK)-MB and NAC isoenzymes (Spinreact, Spain), creatine kinase (CK), γ-glutamyl transpeptidase (γ-GT), lactate dehydrogenase (LDH), alanine transaminase (ALT), aspartate transaminase (AST), alkaline phosphatase (ALP), acid phosphatase (ACP), pseudocholinesterase, ceruloplasmin and amylase (Cormay, Poland)], proteins [albumin, total protein, C-reactive protein (CRP), α_1-antitrypsin, immunoglobulins A, M, G and E (IgA, M, G and E), complements C3 and C4, ferritin, transferrin (Cormay, Poland) and β_2-microglobulin (Spinreact, Spain)], lipids [cholesterol, triglycerides (Cormay, Poland), phospholipids, high-density lipoprotein (HDL) and low-density lipoprotein (LDL) (Spinreact, Spain)], electrolytes [calcium, magnesium, iron, phosphorus (Cormay, Poland), sodium, potassium, chloride and zinc (Spinreact, Spain)]. A very brief description is given below.

Bilirubin was converted to colored azobilirubin by diazotized sulfanilic acid. The color intensity is proportional to the bilirubin concentration in the sample and was measured photometrically at 555 nm. Of the two fractions present in serum (*i.e.* bilirubin glucuronide and free bilirubin loosely bound to albumin), only conjugated bilirubin reacts directly in aqueous solution (direct bilirubin), while free bilirubin requires solubilization with dimethylsulphoxide to react (indirect bilirubin). The concentration of indirect bilirubin = total bilirubin − direct bilirubin.

Lactate was oxidized by lactate oxidase to pyruvate and hydrogen peroxide which, in the presence of peroxidase, reacts with *N*-ethyl-*N*-(2-hydroxy-3-sulfopropyl)-3-methylaniline forming a red compound that was measured at 546 and 700 nm. Glucose oxidase catalyzes the oxidation of glucose to gluconic acid. The formed hydrogen peroxide was detected by a chromogenic oxygen acceptor, phenol-4-aminophenazone in the presence of peroxidase. The intensity of the quinone color formed was measured photometrically at 505 nm. Creatinine reacted with alkaline picrate forming a red complex that was measured photometrically at 492 nm. Urea in the sample reacted with *o*-phthalaldehyde in acid medium forming a colored complex that was measured photometrically at 510 nm. Uric acid was oxidized by uricase to allantoin and hydrogen peroxide, and under the influence of peroxidase, 4-aminophenazone and 2,4-dichlorophenol sulfonate formed a red quinoneimine compound that was measured photometrically at 520 nm.

Calcium quantification was based on the formation of a colored complex with *o*-cresolphthalein in alkaline medium that was measured photometrically at 570 nm. Chloride formed a red ferric thiocyanate complex with mercuric thiocyanate that was measured photometrically at 480 nm. Iron was dissociated from a transferring-iron complex in a weakly acid medium. The liberated iron was reduced to ferrous form

by ascorbic acid and formed a colored complex with FerroZine that was measured photometrically at 562 nm. Magnesium formed a colored complex when reacted with magon sulfonate in alkaline solution. The intensity of the color formed is proportional to the magnesium concentration in the sample and was measured photometrically at 546 nm. Phosphorus reacted with molybdic acid forming a phosphomolybdic complex. Its subsequent reduction in alkaline medium produced a blue molybdenum color that was measured photometrically at 710 nm. Potassium ions reacted with sodium tetraphenylboron in a protein-free alkaline medium to produce a finely dispersed turbid suspension of potassium tetraphenylboron. The turbidity produced is proportional to the potassium concentration and was read photometrically at 578 nm. Sodium was determined enzymatically *via* sodium dependent-galactosidase activity with *o*-nitrophenyl-β-galactoside as the substrate. The absorbance at 405 nm of the product *o*-nitrophenyl is proportional to the sodium concentration. Zinc reacted at pH 8.6, in a buffered media, with a specific complexant, 5-Br-PAPS, to form a stable colored complex that was measured photometrically at 560 nm.

Cholesterol produced a colored complex in the presence of peroxidase that was measured photometrically at 505 nm. Phospholipids were hydrolyzed by phospholipase D and the liberated choline was subsequently oxidized by choline oxidase to betaine with the simultaneous production of hydrogen peroxide. In the presence of peroxidase the hydrogen peroxide couples oxidatively the 4-aminophenazone and dichlorophenol to form a quinoneimine dye that is measured photometrically at 505 nm. Triglycerides were converted to glycerol and free fatty acids by lipoprotein lipase. Glycerol was converted to glycerol-3-phosphate and ADP by glycerol kinase and ATP. Glycerol-3-phosphate was then converted by glycerol phosphate dehydrogenase to dihydroxyacetone phosphate and hydrogen peroxide. In the last reaction, hydrogen peroxide reacted with 4-aminophenazone and *p*-chlorophenol in the presence of peroxidase to give a red colored dye that was measured photometrically at 505 nm. HDL and LDL produced a colored complex in the presence of peroxidase that was measured photometrically at 600 nm.

ACP catalyses the hydrolysis of α-naphthyl phosphate liberating α-naphthol and phosphate. The α-naphthol was then coupled with diazotised 4-chloro-2-methylbenzene (Fast Red TR) to form a diazo dye which was measured photometrically at 405 nm. ALP catalyzes the hydrolysis of *p*-nitrophenyl phosphate at pH 10.4, liberating phosphate and *p*-nitrophenol, which was measured photometrically at 405 nm. Amylase hydrolyzes 2-chloro-4-nitrophenyl-α-D-maltotrioside to release 2-chloro-4-nitrophenol and forms 2-chloro-4-nitrophenyl-α-D-maltoside, maltotriose and glucose. The rate of 2-chloro-4-nitrophenol formation is proportional to the activity of amylase present in the sample and was measured photometrically at 405 nm. Pseudocholinesterase hydrolyzes butyrylthiocholine to butyrate and thiocholine. Thiocholine reacts with 5,5′-dithiobis-2-nitrobenzoic acid to form 5-mercapto-2-nitrobenzoic acid, in which the formation rate was measured photometrically at 405 nm. CK catalyzes the reversible transfer of a phosphate group from phosphocreatine to ADP. This reaction is coupled to those catalyzed by hexokinase and glucose-6-phosphate dehydrogenase. The rate of NADPH formation is proportional to the catalytic concentration of CK present in the sample and was measured photometrically at 340 nm. γ-GT catalyzes the transfer of the γ-glutamyl group from γ-glutamyl-*p*-nitroanilide to the acceptor glycylglycine. The rate of 2-nitro-5-aminobenzoic acid formation is proportional to the catalytic concentration of γ-GT present in the sample and was measured photometrically at 405 nm. AST catalyzes the reversible transfer of an amino group from aspartate to α-ketoglutarate forming glutamate and oxalacetate. The oxalacetate produced was reduced to malate by malate dehydrogenase using NADH as the cofactor. ALT catalyzes the reversible transfer of an amino group from alanine to α-ketoglutarate forming glutamate and pyruvate. The pyruvate produced was reduced to lactate by LDH using NADH as the cofactor. This last reaction was also used to measure LDH activity. The rate of decrease in the concentration of NADH is proportional to the activity of AST, ALT and LDH present in the sample and was measured photometrically at 340 nm. Lipase in the presence of colipase, desoxycholate and calcium ions hydrolyses the substrate 1-2-*O*-dilauryl-*rac*-glycero-3-glutaric acid-(6′-methylresorufin)-ester. The rate of methylresorufin formation was measured photometrically at 580 nm.

Total proteins gave an intensive violet-blue complex with copper salts in an alkaline medium that was measured photometrically at 546 nm. Iodide was included as an antioxidant. Albumin in the presence of bromocresol green at a slightly acid pH produced a color change of the indicator from yellow-green to green-blue. The intensity of the color formed is proportional to the albumin concentration in the sample and was measured photometrically at 605 nm.

C3, C4, α_1-antitrypsin, ceruloplasmin, transferrin, CRP, β_2-microglobulin, IgA, IgG, IgM and IgE form insoluble complexes when mixed with respective antibodies. These complexes cause a turbidity change, depending upon C3, C4, α_1-antitrypsin, ceruloplasmin, transferrin, CRP, β_2-microglobulin, IgA, IgG, IgM and IgE concentrations in the sample. The concentrations can be quantified in comparison with a calibrator of known C3, C4, α_1-antitrypsin, ceruloplasmin, transferrin, CRP, β_2-microglobulin, IgA, IgG, IgM and IgE concentrations.

Blood pH was determined using a micro-electronic pH meter (Sigma-Aldrich, St Louis, MO, USA). Certified calibration buffer standards (Sigma-Aldrich, St Louis, MO, USA) were used before each pH analysis.

Data analysis

Quantification and expression data were statistically processed using GraphPad Prism 6. The determined *p* values of statistical significance were examined using the model of linear regression and the Pearson correlation (*r*). An acceptable Pearson correlation value of $r > 0.900$ was considered for posterior analysis. Mathematical models were developed from the 264 hour kinetics, by performing regression analysis using

Tool Analysis Supplement of Microsoft Excel 2013 for Windows, in order to estimate the slope (m) and y-intercept (b) errors. The level of significance was always set to p-values less than 0.05 ($p < 0.05$).

Results

Quantitative pH and kinetic analysis of biochemical parameters

The concentrations of biochemical parameters were analyzed in 20 different human blood samples to establish a potential relationship between these values and the putrefaction time aiming to identify those that present good correlations. A statistically significant increase was observed in the urea concentration between 27.84–33.49 mg dL^{-1} up to 264 h (r = 0.973, $p < 0.001$) (Fig. S1†). The uric acid concentration decreased until 264 h between 3.39–2.80 mg dL^{-1} and showed a strong correlation ($r = -0.980$, $p < 0.001$) with the putrefaction time (Fig. S1†). The total and direct bilirubin concentrations significantly decreased over time from 0.67 to 0.30 mg dL^{-1} and from 0.14 to 0.01 mg dL^{-1}, respectively ($r = -0.964$ and $r = -0.991$, $p < 0.001$) (Fig. S1†). Our data demonstrate that the remaining substrates (*i.e.* glucose, lactate and creatinine) did not correlate linearly with the putrefaction time (Fig. S2†). Among the electrolytes, the calcium concentration decreased significantly and linearly from 8.45 to 3.70 mg dL^{-1} ($r = -0.986$, $p < 0.001$) (Fig. S1†). A statistically significant increase was observed in the iron concentration between 100.72–188.49 μg dL^{-1} over the putrefaction time (r = 0.987, $p < 0.001$) (Fig. S1†). The remaining electrolytes (*i.e.* zinc, sodium, potassium, magnesium and phosphorus) did not correlate linearly (Fig. S2†) or exhibited several fluctuations with the putrefaction time (*i.e.* chloride) (Fig. S3†). Among the lipids (*i.e.* phospholipids, lipoproteins HDL and LDL, triglycerides and cholesterol), we did not observe any linear correlation between each of the parameters and the putrefaction time (Fig. S2†). Of all proteins evaluated in this study, only transferrin and IgM proved to be useful for PMI estimation (Fig. S1†). The transferrin concentration decreased significantly and linearly between 340.64–275.09 mg dL^{-1} ($r = -0.988$, $p < 0.001$) with the putrefaction time. The IgM concentration decreased linearly from 112.37 to 103.00 ($r = -0.967$, $p < 0.001$). The remaining proteins (*i.e.* total protein, albumin, complements C3 and C4, IgA and G, ferritin, β_2-microglobulin, α_1-antitrypsin and CRP) did not correlate linearly (Fig. S2†) or exhibited several fluctuations with the putrefaction time (*i.e.* IgE) (Fig. S3†). The changes in the activity of several enzymes were also evaluated *in vitro*. The AST concentration increased significantly and linearly between 25.23–40.75 U L^{-1} (r = 0.980, $p < 0.001$) over time (Fig. S1†). The CK concentration also increased significantly between 108.95–190.39 U L^{-1} with the putrefaction time (r = 0.968, $p < 0.001$) (Fig. S1†). Our data demonstrate that the remaining enzymes (*i.e.* ALT, amylase, pseudocholinesterase, ALP, CK-MB isoenzyme, γ-GT, LDH and lipase) did not correlate linearly (Fig. S2†) or exhibited several fluctuations with the putrefaction time (*i.e.* ceruloplasmin, ACP and CK-NAC isoenzyme) (Fig. S3†).

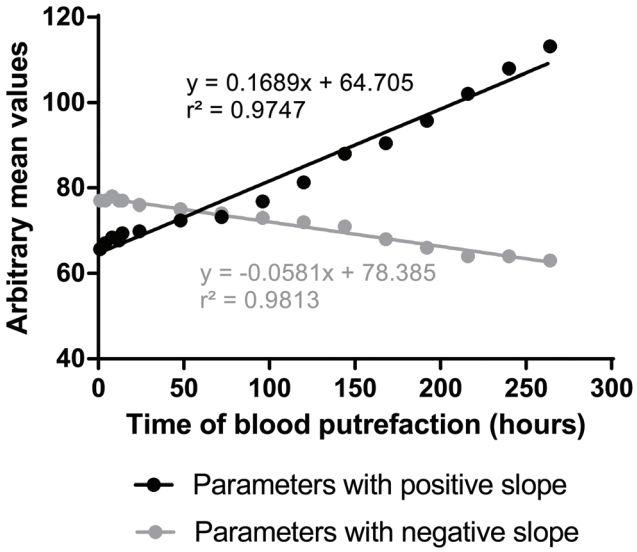

Fig. 1 Mean graphical concentrations of the biochemical parameters (n = 20) analyzed during a 264 hour kinetic period. (A) Parameters with a negative slope (*i.e.* total and direct bilirubin, uric acid, transferrin, immunoglobulin M and calcium); (B) parameters with a positive slope (*i.e.* iron, urea, aspartate transaminase and creatine kinase). The Pearson correlation (r) and p value are depicted.

Aiming to assure the maximum significance between each biochemical parameter and the putrefaction time, we considered for posterior analysis only those with Pearson correlations higher than 0.900 (*i.e.* in absolute value or modulus) and found to be statistically significant (Fig. 1). This approach allowed the identification of 10 potential biochemical parameters in the blood as the most reliable dependent variables that may correlate with the PMI:

- Positive slope – iron, urea, AST and CK;
- Negative slope – total and direct bilirubin, uric acid, transferrin, IgM and calcium.

At each defined endpoint, the samples were also analyzed for pH, since after death several mechanisms may be involved in producing the pH changes.[22] In our study, the pH decreased very slightly in the first 5 days compared to the initial value (pH 7.45–7.10). Afterwards, the pH increased continuously reaching pH 7.74 by the end of the experiment.

Development of a mathematical model with predictive values for PMI estimation

The ultimate goal of this study was to develop a mathematical model to correlate biochemical parameters with the PMI. In that sense, we performed regression analysis with the objective of building descriptive mathematical laws to be used by forensic experts for valid and reliable estimation of the PMI. The linearity of the method was determined by evaluation of the regression curve (biochemical parameter concentration *versus* time) and expressed by the correlation coefficient (r) as pre-

viously proposed.[14] We used 20 independent calibration curves ($y = mx + b$) for each of the 10 selected biochemical parameters to obtain the mean slope (m) and y-intercept (b). Linearity was accepted if $r \geq 0.900$. Nonlinear parameters were excluded from our model. The goal of linear regression was to determine the best estimates for the slope and y-intercept. This was accomplished by minimizing the residual error between the experimental y values, and those values predicted by using a regression line equation. The most commonly used form of linear regression is based on three assumptions: (1) differences between the experimental data and the calculated regression line are due to indeterminate errors affecting the y values, (2) indeterminate errors are normally distributed, and (3) that the indeterminate errors in y do not depend on the value of x. The derivation of equations for calculating the estimated slope and y-intercept can be found elsewhere.[34] This allows us to define regression equations to calculate the PMI using the parameters with positive and negative slopes (Fig. 2, eqn (A) and (B), respectively). Once known, it is possible to determine the PMI and to estimate the error associated with time. For that, we can measure an average signal for our sample ($\bar{Y}_x$) and use it to calculate the value of x. The PMI should be calculated by the mean of the two equations. The standard deviation for the calculated value of x (S_x) is given by the equation in Fig. 2, eqn (C), where K is the number of replicate samples ($K = 20$) used to establish $\bar{Y}_x$, n is the number of measured endpoint times ($n = 16$), $\bar{y}$ is the average signal for each endpoint time, $\sum xx$ is the summation of individual $(x–\bar{x})^2$. Once S_x is known, the confidence interval for the PMI can be calculated assigning the value of t determined by the desired level of confidence ($p < 0.05$) for $n - 2$ degrees of freedom.

A

$$PMI = \frac{(64.71 - |\overline{Y}_X|)}{0.17} \pm 2.16 \times \left[77.60 \times \sqrt{0.08 + \frac{(\overline{Y}_X + 81.84)^2}{3631.78}} \right]$$

B

$$PMI = -\frac{(78.38 - |\overline{Y}_X|)}{0.06} \pm 2.16 \times \left[-73.86 \times \sqrt{0.08 + \frac{(\overline{Y}_X + 72.49)^2}{429.69}} \right]$$

C

$$s_x = \frac{s_y}{m} \sqrt{\frac{1}{K} + \frac{1}{n} + \frac{(\overline{Y}_X - \overline{y})^2}{m^2 \sum xx}}$$

Fig. 2 Mathematical models for the accurate estimation of the PMI. The two equations represent the formula to calculate the PMI using parameters with positive (A) and negative (B) slopes, with a confidence interval of 95% and the standard deviation (C), where ($\bar{Y}_x$) is the average signal for our sample, K is the number of replicate samples used to establish $\bar{Y}_x$, n is the number of measured endpoint times, $\bar{y}$ is the average signal for each endpoint time, $\sum xx$ is the summation of individual $(x–\bar{x})^2$. The mean result of the A and B formulae allows us to determine the PMI.

Discussion

The results of this study allowed us to circumscribe the potential biomarkers (total and direct bilirubin, urea, uric acid, transferrin, immunoglobulin M, creatine kinase, aspartate aminotransferase, calcium and iron) for accurately estimating the PMI. These biochemical parameters were then used to develop mathematical models with predictive values for the accurate estimation of the PMI.

After death, several biochemical alterations occur. Blood glucose concentrations decrease very rapidly after death with a concomitant increase in lactate concentrations.[35–37] Indeed, the *postmortem* lactate concentrations were shown to be up to 60 times higher than *antemortem*.[37] In our study, the lactate concentration progressively increased over time while glucose decreased rapidly up to 144 h. Interestingly, an increased glucose concentration over the remaining putrefaction time was registered. As the human decomposition progresses, cell membranes gradually disintegrate as a result of autolysis and putrefaction processes,[38,39] the *postmortem* glucose concentrations may increase in blood.[40] *In situ*, besides autolysis, glycogen is metabolized to glucose (*i.e.* glycogenolysis namely in liver), which is released into the blood.[40,41] Additionally, glucose may also be formed from non-carbohydrate sources (*e.g.* lactate, amino acids and glycerol) by gluconeogenesis, contributing to the increase in glucose after death.

Creatinine is a degradation product of phosphocreatine (*i.e.* an energy storage molecule in the muscle), which is released into the blood.[41–43] Our study shows that creatinine concentrations increase abruptly until 24 h and then stabilize over the remaining PMI. In previous studies, creatinine showed a tendency to increase in the *postmortem* blood *in situ* up to 48 h.[28] A strong correlation was found in muscle,[44] and there were no significant changes in other specimens such as synovial fluid and vitreous humor.[11]

We found a significant increase in the urea concentration over time, which corroborates other studies performed with the *postmortem* blood.[35,45] However, in other specimens, such as vitreous humor and synovial fluid, urea was shown to remain relatively stable.[9,11] *In situ*, amino acids are oxidized, nitrogen is then released as ammonia and converted mainly to urea in liver, passing into the blood. Upon degradation of pyrimidine bases, the carbon and nitrogen atoms produce carbon dioxide and urea, respectively.[41,43] Thus, an accumulation of ammonia and urea due to amino acid and nucleotide catabolism is a natural consequence of *postmortem* decomposition.[17] Uric acid is also an excretion product containing nitrogen, but is derived from purine bases of nucleic acids and not from proteins.[41] The purine degradation produces hypoxanthine, which is oxidized by xanthine oxidase to uric acid.[1,41] *Postmortem* enzymatic activity is inhibited, since it requires oxygen to function.[17,46,47] In this study, the uric acid concentration decreased linearly with the putrefaction time. However, some previous studies have shown that the blood uric acid remained relatively stable *in vitro* while it decreased in blood *in situ*.[17,48]

The total and direct bilirubin concentrations *in vitro* also significantly and linearly decreased with the putrefaction time. Our results can be explained by the activity of bacterial β-glucuronidases to remove glucuronide groups and then reducing bilirubin (produced by heme oxidation) to urobilinogen and stercobilinogen.[41] Nevertheless, the stability or even a slight increase of total bilirubin was registered during the first 4–5 endpoints. These results are somewhat in accordance with the findings of Uemura and colleagues[28] using right cardiac blood obtained from autopsies. Indeed, these authors observed a non-significant increase in total bilirubin up to 72 h, but they did not extend their study beyond that endpoint. Moreover, cadavers were preserved refrigerated until forensic autopsies and therefore could not be directly compared with our findings. In order to minimize the influence of the preservation time in a refrigerated environment for PMI estimation, blood should be collected quickly after the body is found and not only when the autopsy begins.

Analysis of *postmortem* chemical changes of electrolytes has been extensively studied by several authors with promising results. Indeed, good correlations with PMI have been observed for potassium and sodium, which were shown to increase and decrease respectively, in vitreous humor.[1,10,11,25,49–51] In our study, the potassium concentration increased significantly up to 168 h and decreased over the remaining putrefaction time. The sodium concentration *in vitro* initially remained stable up to 72 h, but decreased significantly with the putrefaction time. Sodium is the most abundant cation in the extracellular space, while potassium is prevalent in the intracellular space.[52] These ions are essential for cellular function, namely for the maintenance of membrane potential and regulation of osmotic pressure.[43,52] After death, cells lose their normal morphology as a result of autolysis and putrefaction processes.[39] Thus, *in vitro*, the increase in extracellular potassium concentration in blood results mainly from loss of potassium from blood cells (namely erythrocytes), and *in situ*, can also result from cells located in the vessels' walls and extravascular tissues.[53] In this study, we found a linear and significant increase in the iron concentration *in vitro* over the putrefaction time. These findings can be explained by the *postmortem* leakage of iron from erythrocytes due to hemolysis and release from transferrin. Accordingly, we observed that the transferrin concentration decreases significantly and linearly with the putrefaction time. The iron storage protein, ferritin,[41,52] initially exhibited an increase, but decreased with the putrefaction time after 72 h.

Other electrolytes such as phosphorus, calcium, magnesium, zinc and chloride have been also studied by some authors mainly in the vitreous humor and synovial fluid.[11,25,54,55] It was demonstrated that the electrolyte concentrations do not change significantly with the putrefaction time. However, others observed a significant correlation between these electrolyte concentrations and the PMI.[4,33,45,56] Our data show that, similar to potassium, the phosphorus concentration increased gradually up to 168 h, but decreased slightly over the remaining putrefaction time. Chloride revealed to be a very unstable parameter over the putrefaction time and therefore was excluded. The magnesium concentration increased *in vitro* up to 96 h and remained practically constant over the remaining putrefaction time. The zinc concentration increased until 120 h and then decreased slightly. The calcium concentration decreased significantly and linearly with the putrefaction time. Calcium plays an important role in the regulation of many cellular processes (*e.g.* blood coagulation, muscle contraction and secretory processes).[41,52] In this regard, we hypothesize that the observed calcium decrease was due to consumption during the coagulation process and was retained in the fibrin coagulum.

Few studies correlate the concentration of lipids with the PMI. The blood lipoproteins HDL and LDL are involved in the transport of lipids from the liver to other tissues in the body.[42,52,57] LDL is the main carrier of lipids (*e.g.* triglycerides and cholesterol) from the liver to peripheral tissues (such as muscle) and to adipose tissue.[52,58] HDL is involved in the reverse transport of lipids from peripheral tissues to the liver.[42,52,58] In our study, the LDL and HDL lipoprotein concentrations initially increase slightly, but then showed a tendency to decrease over time.

The triglyceride concentration *in vitro* showed a tendency to decrease over time. *In situ*, a *postmortem* decrease in the triglyceride concentration was also observed, since these are hydrolyzed in the blood to fatty acids and glycerol by lipoprotein lipase.[41,52] In the adipose tissue, triglycerides are degraded and supply fatty acids and glycerol to the liver and muscle. There they can be used for gluconeogenesis or are directly oxidized.[52] The cholesterol and phospholipid concentrations *in vitro* showed a tendency to increase up to 48 h and then decreased slightly, with some oscillations over time. Sarkioja and colleagues[18] reported that unpredictable fluctuations occur in the plasma triglyceride and cholesterol concentrations within 24 h after death. Previously Uemura *et al.*[28] showed a significant time-dependent decrease in the triglyceride concentration up to 72 h after death and the cholesterol concentration registered some fluctuations.

During the *postmortem* decomposition, proteins are broken down *via* enzymatic processes into proteoses, peptones, polypeptides, and amino acids.[59,60] Liver function is maintained for several hours after death as shown by the ability to carry out protein synthesis at low levels despite *postmortem* conditions.[61] Some authors have proposed PMI estimation based on the effect of the PMI on protein concentrations.[8,28–30,62,63] According to our results, the total protein concentration initially increased, up to 48 h, reaching a plateau that remains unchanged until the end of the experiment. The albumin concentration *in vitro* increased slightly up to 216 h and then decreased over the remaining putrefaction time. β_2-Microglobulin is a protein located on the surface of nucleated cells such as lymphocytes.[52] Our results showed that the β_2-microglobulin concentrations did not change significantly with increasing putrefaction time.

The α_1-antitrypsin concentration decreased during the first 4 h and remained stable over the rest of the experiment.

α_1-Antitrypsin is a circulating protein synthesized by the liver and the most abundant proteinase inhibitor in plasma that downregulates inflammation.[41,52,58] We observed that C-reactive protein, a non-specific indicator of acute phase response in trauma, myocardial infarction, tumors, infection and other inflammatory changes, decreased gradually with the putrefaction time in our experimental setting. The site of this protein synthesis and release is mainly in the liver.[64] Uhlin-Hansen[65] compared the ante- and *postmortem* concentrations of C-reactive protein and reported that the *postmortem* concentration of this protein reduced approximately by 35%. In another study, the C-reactive protein concentration was stable in *postmortem* blood for at least 2 days, suggesting its biochemical stability.[64]

The C3 and C4 complement concentrations increased up to 96 h and decreased over the remaining putrefaction time. The estimation of the PMI based on the third component of C3 cleavage was previously studied in *postmortem* blood, where a significant positive correlation between the percentage of C3 cleavage and PMI was found.[62] Additionally, we observed a decrease in the immunoglobulin G and M concentrations with the putrefaction time. However, the immunoglobulin A concentration remained practically constant up to 120 h, decreasing over the remaining time. E immunoglobulin showed to be a very unstable parameter to be considered for estimation of the putrefaction time.

The determination of enzyme activity for estimation of the PMI was previously presented by some authors.[28,31,32,61,66–69] Some enzymes continue to operate for some time after death (*e.g.* ACP, ALP, esterase, β-glucuronidase), while others rapidly lose their activity (*e.g.* due to pH alterations) within 24–36 h of the start of autolysis (*e.g.* succinic dehydrogenase, cytochrome oxidase).[70,71]

Some hours after death, autolysis releases intracellular enzymes (*e.g.* proteases, lipases, amylases) into the blood.[36] The erythrocytes have high concentrations of AST and LDH enzymes and hemolysis can elevate its *postmortem* concentrations.[66] This study demonstrates that AST increases significantly with the putrefaction time. The ALT concentration also increases, although not significantly, since high concentrations are only found in the liver and kidney. The LDH is an important enzyme, which catalyzes a step in anaerobic glucose metabolism and glucose synthesis in the skeletal muscle, liver and erythrocytes.[17,42] The LDH concentration *in vitro* decreased slightly during the first 24 h and then increased with the putrefaction time. *In situ*, with the tissue decomposition and autolysis (*e.g.* liver and skeletal muscle cells) enzymes leak into the blood and therefore an increase in transaminases, LDH, ALP and ACP concentrations is expected.[41,43] However, in our study, the ALP concentration *in vitro* decreased over time. This enzyme is present in high concentrations in liver, bone, intestine and kidney but not in blood cells,[58] therefore hemolysis of these cells will not have much influence on the concentration and enzyme activity decreases rapidly in the blood. ACP is an enzyme present in the erythrocytes and hemolysis can elevate its concentration in the blood. High concentrations of this enzyme are particularly found in the prostate and liver.[58] In this study, ACP proved to be a very unstable parameter over the putrefaction time. The γ-GT concentration *in vitro* remained relatively stable up to 192 h, decreasing over the remaining putrefaction time. This is a cellular enzyme that is particularly present in high levels in the liver, kidney and pancreas.[58] γ-GT shows a tendency to increase towards *postmortem* in a time-dependently manner, though not significantly in *postmortem* blood.[11]

We also found that the CK concentration correlates significantly with the putrefaction time. The concentration of CK-MB isoenzyme increases slightly up to 96 h and is more pronounced over the remaining putrefaction time. The CK-NAC isoenzyme proved to be a very unstable parameter for PMI estimation. CK is found in higher concentrations in the muscle cells. CK catalyzes the transfer of phosphate from adenosine triphosphate to creatinine, to form phosphocreatinine. The *in vitro* results demonstrated that this enzyme remained active over time, since the creatinine is a degradation product from phosphocreatinine and increased over time. *In situ*, there is an increase in the CK (namely MB isoenzyme of CK) *postmortem* concentration due to the release of this enzyme into the blood from cell lysis in the heart muscle and necrotic tissue after death. *In vitro*, the ceruloplasmin was also an unstable parameter over the putrefaction time. Ceruloplasmin is a serum enzyme that contains copper, synthesized mainly by the hepatic cells and is involved in the oxidation of iron so it can be transported.[41,43]

The amylase concentration was relatively stable *in vitro* up to 120 h, decreasing significantly over the remaining time. The amylase enzyme is produced mainly by pancreas and salivary glands. This enzyme may leak into the blood due to the lysis of pancreatic cells, being expected and increases in the *postmortem* concentration *in situ*. The lipase concentration *in vitro* decreased slightly and remained relatively stable up to 264 h, with some oscillations over time. Lipase is a pancreatic enzyme that hydrolyzes triglycerides to fatty acids and glycerol.[41,52] Pseudocholinesterase is an enzyme that is present in blood, but it is synthesized in the liver. *In vitro*, the pseudocholinesterase concentration remained practically constant up to 216 h and decreased over the remaining time. In a previous study[28] this enzyme showed a tendency to decrease in a time-dependent manner in *postmortem* blood.

At each defined endpoint, the blood samples were also analyzed for pH, since after death several mechanisms (*e.g.* autolysis, putrefaction) may be involved, resulting in pH modifications.[22] In our study, the pH decreased very slightly compared to initial values (pH 7.45 to 7.10) and then increased to 7.74 until the limit of our study. Similarly, Donaldson and Lamont[17] performed an *in vitro* study with blood samples from rats and humans and verified that the pH only decreased slightly (pH 7.4 to 7.1) in comparison with an *in situ* study (pH 7.4 to 5.1) over a 96 hour period. Our hypothesis is that, *in vitro*, the autolysis and putrefactive processes do not occur as extensively as *in situ* and consequently the blood cells are degraded more slowly over time. In cadavers,

several compounds are released into the blood resulting from the putrefactive alterations in organs. Therefore, the accumulation of acidic metabolites is much more significant *in situ* and the blood pH decreases more rapidly. This decline in pH values does not continue indefinitely. Indeed, it was also previously reported that the pH starts to rise after approximately four days.[19,71,72]

The results of this study impelled us to develop a mathematical model to describe the behavior of the identified biochemical parameters over the PMI as a valuable tool for forensic pathologists. Only total and direct bilirubin, urea, uric acid, transferrin, IgM, CK, AST, calcium and iron biochemical parameters were considered, since Pearson correlations were higher than 0.900 (*i.e.* in absolute value or modulus). For the purpose of generating the formulae to estimate the PMI, the mean concentrations of parameters with a negative slope (*i.e.* total and direct bilirubin, uric acid, transferrin, IgM and calcium) and the mean concentrations of parameters with a positive slope (*i.e.* iron, urea, AST and CK) were calculated. Thus, two formulae were generated. For estimating the PMI in real samples, the average signals obtained from selected parameters with positive and negative slopes ($\bar{Y}_x$) are used to calculate the value of x. The PMI should be calculated by the mean of the two equations. This mathematical model can thus be considered a promising easy approach for PMI estimation.

Conclusions

It is expected that the current study may provide a new paradigm for estimation of the PMI and become a complementary procedure for the methodologies already used. It is important to mention that the proposed model can match the most commonly found environmental conditions after death. Indeed, we followed the *postmortem* decline of the body temperature model previously described by Siegel.[13] However, this model is influenced by internal (or intrinsic) and external (or extrinsic) antemortem and *postmortem* conditions. Age (*e.g.* low fluid levels of elderly inhibit the growth of microorganisms and delays decomposition), gender (*e.g.* abundant subcutaneous fatty tissue of females retains body heat for a longer period and decomposition is accelerated), xenobiotic administration, cause of death (*e.g.* hanging may influence the levels of potassium and hypoxanthine in vitreous humor), body mass (*e.g.* an obese will form adipocere more readily and thus delays the decomposition) and duration of the agonal state are some internal factors that may influence the estimation of the PMI.[3–5] Regarding external factors, environment temperature, humidity, rain, clothing (acts as a barrier that delays decomposition), location of the body (*e.g.* a body buried in soil is less influenced by oxidative processes by the lack of oxygen and will decompose at a significantly slower rate than if exposed to air) and insect or animal activity have been reported to influence the estimation of the PMI.[6–8] Therefore, the initial value as well as the slope of the curve will depend on many factors, which means that estimation of the time since death only reveals a certain period of time, but not a precise time point. Nevertheless, it was impossible to attain all potential variables and therefore this represents a preliminary study that must be further validated using laboratory animals and then with human *in situ* samples.

Acknowledgements

Ricardo Dinis-Oliveira acknowledges Fundação para a Ciência e a Tecnologia (FCT) for his Investigator Grant (IF/01147/2013).

References

1 M. L. Passos, A. M. Santos, A. I. Pereira, *et al.*, Estimation of postmortem interval by hypoxanthine and potassium evaluation in vitreous humor with a sequential injection system, *Talanta*, 2009, **79**, 1094–1099.
2 B. Madea, *Handbook of Forensic Medicine*, John Wiley & Sons, Ltd, Oxford, 2014.
3 B. L. Zhu, T. Ishikawa, T. Michiue, *et al.*, Differences in postmortem urea nitrogen, creatinine and uric acid levels between blood and pericardial fluid in acute death, *Leg. Med.*, 2007, **9**, 115–122.
4 D. Singh, R. Prashad, C. Parkash, S. K. Sharma and A. N. Pandey, Double logarithmic, linear relationship between plasma chloride concentration and time since death in humans in Chandigarh Zone of North-West India, *Leg. Med.*, 2003, **5**, 49–54.
5 B. Madea and F. Musshoff, Postmortem biochemistry, *Forensic Sci. Int.*, 2007, **165**, 165–171.
6 M. T. Ferreira and E. Cunha, Can we infer post mortem interval on the basis of decomposition rate? A case from a Portuguese cemetery, *Forensic Sci. Int.*, 2013, **226**, 298e1–298e6.
7 A. A. Vass, The elusive universal post-mortem interval formula, *Forensic Sci. Int.*, 2011, **204**, 34–40.
8 Y. O. Poloz and D. H. O'Day, Determining time of death: temperature-dependent postmortem changes in calcineurin A, MARCKS, CaMKII, and protein phosphatase 2A in mouse, *Int. J. Leg. Med.*, 2009, **123**, 305–314.
9 J. I. Munoz Barus, M. Febrero-Bande and C. Cadarso-Suarez, Flexible regression models for estimating postmortem interval (PMI) in forensic medicine, *Stat. Med.*, 2008, **27**, 5026–5038.
10 J. I. Munoz, J. M. Suarez-Penaranda, X. L. Otero, *et al.*, A new perspective in the estimation of postmortem interval (PMI) based on vitreous, *J. Forensic Sci.*, 2001, **46**, 209–214.
11 N. K. Tumram, R. V. Bardale and A. P. Dongre, Postmortem analysis of synovial fluid and vitreous humour for determination of death interval: A comparative study, *Forensic Sci. Int.*, 2011, **204**, 186–190.

12 B. Madea, Is there a recent progress in the estimation of postmortem interval by means of thanatochemistry?, *Forensic Sci. Int.*, 2005, **151**, 139–149.
13 J. A. Siegel, P. J. Saukko and G. C. Knupfer, *Encyclopedia of Forensic Sciences*, Academic Press, London, 2000.
14 F. Sampaio-Silva, T. Magalhaes, F. Carvalho, R. J. Dinis-Oliveira and R. Silvestre, Profiling of RNA degradation for estimation of post morterm interval, *PLoS One*, 2013, **8**, e56507.
15 A. A. Vass, S. A. Barshick, G. Sega, *et al.*, Decomposition chemistry of human remains: a new methodology for determining the postmortem interval, *J. Forensic Sci.*, 2002, **47**, 542–553.
16 S. Sasaki, S. Tsunenari and M. Kanda, The estimation of the time of death by non-protein nitrogen (NPN) in cadaveric materials, Report 3: multiple regression analysis of NPN values in human cadaveric materials, *Forensic Sci. Int*, 1983, **22**, pp. 11–22.
17 A. E. Donaldson and I. L. Lamont, Biochemistry Changes That Occur after Death: Potential Markers for Determining Post-Mortem Interval, *PLoS One*, 2013, **8**, e82011.
18 T. Sarkioja, S. Yla-Herttuala, T. Solakivi, T. Nikkari and J. Hirvonen, Stability of plasma total cholesterol, triglycerides, and apolipoproteins B and A-I during the early postmortem period, *J. Forensic Sci.*, 1988, **33**, 1432–1438.
19 V. A. Boumba, K. S. Ziavrou and T. Vougiouklakis, Biochemical pathways generating post-mortem volatile compounds co-detected during forensic ethanol analyses, *Forensic Sci. Int.*, 2008, **174**, 133–151.
20 A. L. Lehninger, *Principles of Biochemistry*, Worth Publishers, New York, 1982.
21 M. Statheropoulos, A. Agapiou, C. Spiliopoulou, G. C. Pallis and E. Sianos, Environmental aspects of VOCs evolved in the early stages of human decomposition, *Sci. Total Environ.*, 2007, **385**, 221–227.
22 W. R. Sawyer, D. R. Steup, B. S. Martin and R. B. Forney, Cardiac blood pH as a possible indicator of postmortem interval, *J. Forensic Sci.*, 1988, **33**, 1439–1444.
23 B. Madea, C. Kreuser and S. Banaschak, Postmortem biochemical examination of synovial fluid–a preliminary study, *Forensic Sci. Int.*, 2001, **118**, 29–35.
24 J. I. Munoz-Barus, J. Suarez-Penaranda, X. L. Otero, *et al.*, Improved estimation of postmortem interval based on differential behaviour of vitreous potassium and hypoxantine in death by hanging, *Forensic Sci. Int.*, 2002, **125**, 67–74.
25 K. D. Jashnani, S. A. Kale and A. B. Rupani, Vitreous humor: biochemical constituents in estimation of postmortem interval, *J. Forensic Sci.*, 2010, **55**, 1523–1527.
26 M. J. Prieto-Castello, J. P. Hernandez del Rincon, C. Perez-Sirvent, *et al.*, Application of biochemical and X-ray diffraction analyses to establish the postmortem interval, *Forensic Sci. Int.*, 2007, **172**, 112–118.
27 E. Lendoiro, C. Cordeiro, M. S. Rodriguez-Calvo, *et al.*, Applications of Tandem Mass Spectrometry (LC-MSMS) in estimating the post-mortem interval using the biochemistry of the vitreous humour, *Forensic Sci. Int.*, 2012, **223**, 160–164.
28 K. Uemura, K. Shintani-Ishida, K. Saka, *et al.*, Biochemical blood markers and sampling sites in forensic autopsy, *J. Forensic Leg. Med.*, 2008, **15**, 312–317.
29 S. Kang, N. Kassam, M. L. Gauthier and D. H. O'Day, Postmortem changes in calmodulin binding proteins in muscle and lung, *Forensic Sci. Int.*, 2003, **131**, 140–147.
30 A. J. Sabucedo and K. G. Furton, Estimation of postmortem interval using the protein marker cardiac Troponin I, *Forensic Sci. Int.*, 2003, **134**, 11–16.
31 H. Ikegaya, H. Iwase, K. Hatanaka, *et al.*, Postmortem changes in cytochrome c oxidase activity in various organs of the rat and in human heart, *Forensic Sci. Int.*, 2000, **108**, 181–186.
32 T. Gos and S. Raszeja, Postmortem activity of lactate and malate dehydrogenase in human liver in relation to time after death, *Int. J. Leg. Med.*, 1993, **106**, 25–29.
33 A. Mathur and Y. K. Agrawal, An overview of methods used for estimation of time since death, *Austr. J. Forensic Sci.*, 2011, **43**, 275–285.
34 N. R. Draper and H. Smith, *Applied Regression Analysis*, Wiley, New York, 3rd edn, 1998.
35 H. N. Naumann, Postmortem chemistry of the vitreous body in man, *AMA Arch. Ophthalmol.*, 1959, **62**, 356–363.
36 A. R. Forrest, Obtaining samples at post mortem examination for toxicological and biochemical analyses, *J. Clin. Pathol.*, 1993, **46**, 292–296.
37 M. Z. Karlovsek, Diagnostic values of combined glucose and lactate values in cerebrospinal fluid and vitreous humour–our experiences, *Forensic Sci. Int.*, 2004, **146** (Suppl), S19–S23.
38 F. C. Kugelberg and A. W. Jones, Interpreting results of ethanol analysis in postmortem specimens: a review of the literature, *Forensic Sci. Int.*, 2007, **165**, 10–29.
39 H. Dokgoz, N. Arican, I. Elmas and S. K. Fincanci, Comparison of morphological changes in white blood cells after death and in vitro storage of blood for the estimation of postmortem interval, *Forensic Sci. Int.*, 2001, **124**, 25–31.
40 J. E. Corry, A review. Possible sources of ethanol ante- and post-mortem: its relationship to the biochemistry and microbiology of decomposition, *J. Appl. Bacteriol.*, 1978, **44**, 1–56.
41 M. A. Lieberman and R. Ricer, *Biochemistry, Molecular Biology, and Genetics*, Lippincott Williams & Wilkins, Philadelphia, 2014.
42 J. M. Berg, J. L. Tymoczko and L. Stryer, *Biochemistry*, W. H. Freeman and Company, New York, 2012.
43 J. W. Pelley, *Elsevier's Integrated Biochemistry*, Mosby, Elsevier, Philadelphia, 2007.
44 F. Brion, B. Marc, F. Launay, J. Gailledreau and M. Durigon, Postmortem interval estimation by creatinine levels in human psoas muscle, *Forensic Sci. Int.*, 1991, **52**, 113–120.
45 R. Drolet, S. D'Allaire and M. Chagnon, The evaluation of postmortem ocular fluid analysis as a diagnostic aid in sows, *J. Vet. Diagn. Invest.*, 1990, **2**, 9–13.
46 G. Bocaz-Beneventi, F. Tagliaro, F. Bortolotti, G. Manetto and J. Havel, Capillary zone electrophoresis and artificial

neural networks for estimation of the post-mortem interval (PMI) using electrolytes measurements in human vitreous humour, *Int. J. Leg. Med.*, 2002, **116**, 5–11.

47 B. Madea, H. Käferstein, N. Hermann and G. Sticht, Hypoxanthine in vitreous humour and cerebrospinal fluid - a marker of postmortem interval and prolonged (vital) hypoxia? Remarks also on hypoxanthine in SIDS, *Forensic Sci. Int.*, 1994, **65**, 19–31.

48 B. L. Zhu, K. Ishida, L. Quan, *et al.*, Postmortem serum uric acid and creatinine levels in relation to the causes of death, *Forensic Sci. Int.*, 2002, **125**, 59–66.

49 A. Mulla and J. Kalra, Vitreous Humour Biochemical Constituents - Evaluation of eye differences, *Am. J. Forensic Med. Pathol.*, 2005, **26**, 146–149.

50 B. Madea, C. Henssge, W. Honig and A. Gerbracht, References for determining the time of death by potassium in vitreous humor, *Forensic Sci. Int.*, 1989, **40**, 231–243.

51 B. A. Balasooriya, C. A. St Hill and A. R. Williams, The biochemistry of vitreous humor. A comparative study of the potassium, sodium and urate concentrations in the eyes at identical time intervals after death, *Forensic Sci. Int.*, 1984, **26**, 85–91.

52 G. Michal and D. Schomburg, *Biochemical Pathways: An Atlas of Biochemistry and Molecular Biology*, John Wiley & Sons, Inc., Canada, 2012.

53 D. Querido, In vitro loss of potassium from erythrocytes during the 0–108 h postmortem period in rats: relationship between potassium loss and postmortem interval, *Forensic Sci. Int.*, 1991, **51**, 111–123.

54 B. Madea, N. Hermann and C. Henssge, Calcium concentration in vitreous humor–a means for determining time of death?, *Beitr. Gerichtl. Med.*, 1990, **48**, 489–499.

55 J. G. Farmer, F. Benomran, A. A. Watson and W. A. Harland, Magnesium, potassium, sodium and calcium in post-mortem vitreous humour from humans, *Forensic Sci. Int.*, 1985, **27**, 1–13.

56 D. Querido, Linearization of the relationship between postmortem plasma chloride concentration and postmortem interval in rats, *Forensic Sci. Int.*, 1990, **45**, 117–127.

57 J. A. Timbrell, *Principles of Biochemical Toxicology*, Informa Healthcare Inc., USA, 2009.

58 K. Wilson and J. Walker, *Principles and Techniques of Biochemistry and Molecular Biology*, Cambridge University Press, United Kingdom, 2010.

59 E. M. Hoffman, A. M. Curran, N. Dulgerian, R. A. Stockham and B. A. Eckenrode, Characterization of the volatile organic compounds present in the headspace of decomposing human remains, *Forensic Sci. Int.*, 2009, **186**, 6–13.

60 J. Dekeirsschieter, F. J. Verheggen, M. Gohy, *et al.*, Cadaveric volatile organic compounds released by decaying pig carcasses (Sus domesticus L.) in different biotopes, *Forensic Sci. Int.*, 2009, **189**, 46–53.

61 W. C. Nunley, K. E. Schuit, M. W. Dickie and J. B. Kinlaw, Delayed, in vivo hepatic post-mortem autolysis, *Virchows Arch. B*, 1972, **11**, 289–302.

62 Y. Kominato, S. Harada, K. Yamazaki and S. Misawa, Estimation of postmortem interval based on the third component of complement (C3) cleavage, *J. Forensic Sci.*, 1988, **33**, 404–409.

63 M. Miura, T. Naka and S. Miyaishi, Postmortem changes in myoglobin content in organs, *Acta Med. Okayama*, 2011, **65**, 225–230.

64 M. Q. Fujita, B. L. Zhu, K. Ishida, L. Quan, S. Oritani and H. Maeda, Serum C-reactive protein levels in postmortem blood–an analysis with special reference to the cause of death and survival time, *Forensic Sci. Int.*, 2002, **130**, 160–166.

65 L. Uhlin-Hansen, C-reactive protein (CRP), a comparison of pre- and post-mortem blood levels, *Forensic Sci. Int.*, 2001, **124**, 32–35.

66 K. L. Buras, *Are Enzymes Accurate Indicators of Postmortem Interval? A Biochemical analysis*, Louisiana State University, B.S., 2006.

67 A. Kooij, M. Schijns, W. M. Frederiks, C. J. Van-Noorden and J. James, Distribution of xanthine oxidoreductase activity in human tissues–a histochemical and biochemical study, *Virchows Arch. B*, 1992, **63**, 17–23.

68 S. Fahn and L. J. Cote, Stability of enzymes in post-mortem rat brain, *J. Neurochem.*, 1976, **26**, 1039–1042.

69 J. T. Karkela, Critical evaluation of postmortem changes in human autopsy cisternal fluid, Enzymes, electrolytes, acid–base balance, glucose and glycolysis, free amino acids and ammonia, Correlation to total brain ischemia, *J. Forensic Sci.*, 1993, **38**, 603–616.

70 W. E. D. Evans, *The Chemistry of Death*, Charles C Thomas, Springfield, 1963.

71 D. M. Butzbach, The influence of putrefaction and sample storage on post-mortem toxicology results, *Forensic Sci., Med., Pathol.*, 2010, **6**, 35–45.

72 F. Schleyer, Determination of the time of death in the early post-mortem interval, in: *Methods of Forensic Science*, ed. F. Lindquist, Interscience Publishers, New York, 1963.